Redondo, J.; Sánchez Pérez, JV.; Blasco, X.; Herrero Durá, JM.; Vorlander, M. (2016). Optimized sound diffusers based on sonic crystals using a multiobjective evolutionary algorithm. Journal of the Acoustical Society of America. 139(5):2807-2814. doi:10.1121/1.4948580.

Optimized Sound Diffusers based on Sonic Crystals

J. Redondo[(1)], J. V. Sánchez-Pérez[(1)], X. Blasco[(1)], J. M. Herrero[(1)], M. Vorländer[(2)]

[(1)] Universitat Politècnica de València, Camino de Vera S/N, 46022 Valencia, Spain

[(2)] Institut für Technische Akustik. RWTH Aachen University

Abstract

Sonic crystals have been demonstrated to be good candidates to substitute conventional diffusers in order to overcome the need for extremely deep structures when low frequencies have to be scattered. In this work, the possibility of optimizing such structures providing better performance over a large frequency range is explored. For doing so, multiobjective evolutionary algorithms have been used in combination with a Finite-Difference Time-Domain (FDTD) algorithm that allow predicting the performance of a sound diffuser. The results provided by the multiobjective algorithm, show that diffusion can be significantly increased. Additionally the multiobjective optimization is compared with conventional optimizations in which a single objective quantifies the performance of sound diffusers.

I. INTRODUCTION

Four decades after the invention of sound diffusers by Schroeder [1] is fairly well demonstrated their performance in increasing the sound diffuseness, in elimination of flutter echoes or in reducing coloration phenomena [2]. During these years, several authors have suggested alternatives to the first proposals of Schroeder, using different numerical sequences to design the depth of the wells [3], changing the classic stepped diffusers by more attractive shapes [4], or replacing the different depths of the wells by an irregular mesh of reflective or absorptive small areas [5].

In phase diffusers, defined as diffusers made with a set of wells of different depths, the lowest frequency at which significant diffusion occurs is determined by the maximum depth of the set. This means that to be effective in the low frequency range, i.e. 125Hz and 250Hz octave bands, phase diffusers require a depth of about one meter. To overcome this limitation, new composite materials, called Sonic Crystals (SC), have been proposed to work as diffusers in the range of low frequencies without the need for extremely deep structures [6]. SC can be defined as periodic arrays of isotropic scatterers embedded in isotropic elastic backgrounds, being one of them a fluid [7-8]. A frequently used two-dimensional SC is formed by cylindrical rigid scatterers arranged in square or triangular lattices and surrounded by air. The potential use of SC as diffusers is closely related to one of their most interesting features, which is the existence of sonic band gaps, defined as ranges of frequencies where the sound cannot propagate through the SC. The existence of band gaps is the result of the interference of waves due to a multiple scattering process within the SC, appearing when the wavelength is of the order of the spatial period of the SC. The scale of the structure is then determined by the wavelength of the sound wave, and consequently by the sound frequencies of interest. As a result, size has been for years the main limitation in the use of SC for audible applications, since extremely large structures are required to observe effects at audible frequencies. However, in last years the diffusive properties of SC have been considered [9], and this fact has led to the use of such structures as acoustic scattering devices with high diffusion coefficient at low frequency ranges [6].

Evolutionary algorithms have been used as optimization techniques to design technologically advanced devices based on SC or to increase some structural properties of such materials. Thus the band gap properties have been increased, using multiobjective evolutionary algorithms, to design acoustic barriers [10-12]. In these optimization processes, two objective functions have been defined in order to ensure the maximum attenuation in the frequency range analyzed: the mean acoustic pressure and the mean deviation of the acoustic pressure in the selected point. Moreover, some authors have used these algorithms, but considering a single-objective function, to propose the construction of different acoustic lenses generated by inverse design. In this last case, the objective function optimized has been the acoustic pressure in the focal point [13-14].

On the other hand, the application of optimization techniques in the field of sound diffusers is partially unexplored. In 1995 Cox [15] suggested the use of iterative methods as downhill simplex and quasi-Newton methods to optimize phase diffusers with quite good results. The objective function used was a parameter to estimate the diffusion, defined as the standard error of the sound pressure over the measurement positions, averaged over the desired working frequency range. In order to avoid low performance for particular frequencies within that range, a penalty was introduced adding the standard error to the frequency averaging.

Optimization processes have also been used in the case of the design of commercial diffusers based on curved surfaces. The basic idea is to optimize the shape of curved surfaces to act as diffusers, fulfilling the requirements of both visual aesthetics and good acoustic performance. In the design process, it is necessary to obtain a set of numbers that describe the shape of the curved surface. These shape parameters can be obtained using different mathematical representations as Fourier series or cubic spline algorithms. In all cases, a predetermined number of critical points of the problem surface, which can vary their position depending on the diffusion performance of the surface, have to be selected. The optimum set of positions of the different critical points provide the desired curved surface diffuser. The optimization can be done by using different single-objective functions, as the diffusion parameter defined above [3].

Finally, volumetric diffusers based on SC have been designed using evolutionary algorithms with a single-objective function, the standard diffusion coefficient, along to a two-dimensional Fourier approximation, creating arrays with a high diffusion performance [9]. In all these named cases the optimization has been carried out by either removing randomly or varying the diameter of the rigid cylinders that form the different SC.

As a conclusion, multiobjective evolutionary algorithms have never been used in the field of acoustic diffusers neither in the case of the phase diffusers nor in the case of those based on SC. Therefore, the goal of this paper is the design of Optimized Sonic Crystal Sound Diffusers (OSCSD) to create devices that work properly in the range of low frequencies (octave bands centered at 125Hz and 250Hz) with a reasonable size, using multiobjective evolutionary algorithms. Moreover, we provide here a study of the robustness of the solutions obtained, developing tools that can help to make a decision about the choice of the most appropriated diffuser. To do that, we will consider as the starting design of the optimization process the Sonic Crystal Sound Diffuser (SCSD) proposed by Redondo et al. [6], designed to work in the range of low frequencies. This SCSD is composed by a bi-periodic structure formed by a set of 45x4 cylindrical scatterers with radius equal to 3.5cm, arranged in a square array with alternative lattice constants a=8.8cm and a=7.2cm.

The paper is organized as follows: in section 2 we describe the optimization process. The results are analyzed and discussed in section 3. Section 4 will explore a new possibility for the selection of optimal individuals. In Section 5, multi-objective optimization is compared to single-objective optimization. Last section contains the concluding remarks, where the main conclusions are summarized.

II. DESCRIPTION OF THE OPTIMIZATION PROCESS

The starting point of this paper is the Bi-Periodic Sound Diffuser (BPD) based on Sonic Crystals presented in [6] (see Figure 1a). That device has a high performance in the low frequency range without the need for large depth. However, it can be largely improved by evolutionary algorithms. For doing so, a gene codification must be established. The possible candidates will be encoded by a set of genes that represent in our case a set of 180 normalized cylinders radii. We have considered here that the radii of the cylinders can take six different values from 0 to 1 with steps of 0.2, where 0 means that the cylinder does not exist and 1 is the maximum radius that can be used, which is given by half the lattice constant. So, an individual θ is represented by a genotype given by a vector of length 180, varying each element from 0 to 1. Figure 1 illustrates the codification of a portion of the Sonic Crystal.

A Quantification of the performance of sound diffusers

Next step is to propose Cost Functions that can be used by an evolutionary algorithm to quantify the performance of each candidate. There are basically two methods to quantify the performance of sound diffusers, both standardized by the International Organization for Standardization (ISO).

The first method to quantify the performance of sound diffusers (ISO 17497-Part 1) [16] allows the direct extraction of the so-called scattering coefficient, under the assumption that scattered sound is incoherent. A test sample is introduced into a reverberant chamber, and several impulse responses for different sample orientations are obtained. Using synchronous averaging of these measurements, the diffuse reflected sound is eliminated, and a virtual impulse response is obtained. A pseudo-absorption-coefficient can be obtained from the virtual impulse response in an analogous way to the Sabine method [17]. Finally, a scattering coefficient is obtained from this pseudo-absorption coefficient.

An alternative method is standarized by ISO 17497 – Part 2 [18]. This standard is based on the measurement of the reflected sound over a predetermined range of angles, in a similar way than the directivity measurement of loudspeakers. For this purpose, an impulse response of the sample must be obtained. To do that, a microphone is moved along a semi-circumference (or over a hemisphere for full three dimensional evaluation), centered on the middle point of the test sample. For a complete characterization of the diffuser, the incidence angle is varied from –90º to 90º. Direct sound should be eliminated by appropriate windowing of the signal. Large anechoic environments are needed to ensure far field conditions. The parameter measured using this technique is known as the diffusion coefficient and is defined as follows:

$$d'_j = \frac{\left(\sum_{i=1}^{n} p_{ij}^2\right)^2 - \sum_{i=1}^{n}\left(p_{ij}^2\right)^2}{(n-1)\sum_{i=1}^{n}\left(p_{ij}^2\right)^2} \qquad (1)$$

where d'_j is the diffusion coefficient for the j-th one-third octave band considered, p_{ij} is the sound pressure of the reflected sound for the j-th one-third octave band at the i-th measurement position, and n is the number of measurement positions. To normalize this diffusion coefficient from zero to one, d'_j is compared with a flat surface that is considered the worst case. Thus, the normalized diffusion coefficient, d_j, is defined as:

$$d_j = \frac{d'_j - d_{j,ref}}{1 - d_{j,ref}} \qquad (2)$$

where d_j is the normalized diffusion coefficient for the j-th one-third octave band, and $d_{j,ref}$ is the diffusion coefficient of a flat panel for the j-th one-third octave band. As a result, d_j is equal to zero for flat surfaces.

Both characterization techniques can be simulated with algorithms based on the two-dimensional Finite Difference Time Domain (FDTD) method [19-20]. However, simulations following the second characterization method are much faster than the ones carried out following the first one. So, we have chosen the second standard to simulate all the structures considered in the present paper. Further details about the FDTD set up used in this paper can be found in [19].

Next, a set of Cost Functions J(θ) have to be defined to perform the optimization process. Notice that an optimization process seeks to minimize at least one cost function. Generally speaking, the number of Cost Functions in an optimization process is not limited, but the computational time can be greatly enhanced when increasing their number.

Our target here is to improve the performance of diffusers based on SC for low frequencies, where the use of conventional diffusers implies high depths of the wells (around 1 m for 100 Hz one-third octave band) making its use impractical. Therefore, we have focused our attention in the so-called low frequency range, which includes six one-third octave bands (100Hz, 125Hz, 160Hz, 200Hz, 250Hz and 315 Hz) that in the following will be numbered from one to six. Once the general target of our optimization process has been fixed, the choice of the specific Cost Functions represents the key of the success in the obtaining of the optimal solutions. Actually, there are not global rules about the choice of these Cost Functions but the final choice depends on the actual problem to be solved by the diffuser.

To maximize the performance of Sonic Crystals Sound Diffusers in the low frequency range, we suggest five Cost Functions. All the Cost Functions are defined to be zero for the best case. Although we have chosen these five functions, we would like to highlight the flexibility of the approach concerning the target and the frequency content of the acoustic signal, because the final choice in the optimization process will depend on the particular problem to be solved by the diffusor. It might be a specific normal mode in recording studio, which should be destroyed by scattering, while the signal has a broadband frequency spectrum. Or it might be a specific treatment for a focus in a dome at a given frequency of a narrowband signal.

The first Cost Function that we suggest corresponds to the overall average of the normalized diffusion coefficient, namely:

$$J_{\mathrm{low}}(\theta) = 1 - \bar{d} = 1 - \sum_{j=1}^{m} \left|\frac{d_j(\theta)}{m}\right| \qquad \text{with m=6} \qquad (3)$$

The danger when using this cost function alone, is that diffusion can be very uneven versus frequency. In other words, frequencies with very good diffusion may compensate for frequencies with very poor diffusion. This problem can be easily solved by introducing an additional Cost Function that evaluates the variability of diffusion over the frequency range of interest. Our suggestion is to use the standard deviation, i.e.:

$$J_{\mathrm{varlow}}(\theta) = \sqrt{\frac{\sum_{j=1}^{m}(\bar{d}-|d_j(\theta)|)^2}{m-1}} \qquad \text{with m=6} \qquad (4)$$

These two Cost Functions are similar to the ones used by Cox in [15]. The main objective function was the standard error of the sound pressure over the measurement positions, averaged over the desired working frequency range. The second one was the standard error of the first parameter over the frequency range of optimization. In that work both parameters were added to get a single Cost Function. We will compare both approaches in section 5, Discussion.

Two additional Cost Functions are defined in order to estimate separately the performance of candidates in the two octave bands within the low frequency range, i.e., 125Hz and 250 Hz octave bands. Both octave bands are obtained from the values of the one third octave bands considered.

$$J_{125}(\theta) = 1 - \overline{d_{125}} = 1 - \sum_{j=1}^{3} \left| \frac{d_j(\theta)}{3} \right| \qquad (5)$$

$$J_{250}(\theta) = 1 - \overline{d_{250}} = 1 - \sum_{j=4}^{6} \left| \frac{d_j(\theta)}{3} \right| \qquad (6)$$

Finally, to illustrate the case in which high diffusion is needed in a particular narrow frequency range, we suggest a Cost Function that considers only a particular one third octave band. Without loss of generality, we will consider in this paper the lowest frequency, i.e. 100 Hz one third octave band:

$$J_{100}(\theta) = 1 - d_1 \qquad (7)$$

In the optimization process followed, we have considered three pairs of Cost Functions in order to consider the problem as a multi-objective optimization: J_{low}&J_{varlow}; J_{125}&J_{250}; and finally J_{low}&J_{100}.

B. Multi-objective evolutionary algorithm

Once described the codification and the Cost Functions, in this subsection we will briefly describe the Evolutionary algorithm used in the present work. A multiobjective optimization (MO) [21-22] is chosen in order to attain solutions that satisfy several conflicting objectives simultaneously. In general, when several objectives have to be satisfied, improvements in one of them produce a degradation of the others. That means there is no an unique solution, and a general way to solve the proposed problem is to localize the set of optimal solutions known as Pareto set, which is mapped to the objective space as the Pareto front. The final step in the MO resolution is to select one of these optimal solution according to designer preferences.

A general basic multiobjective problem can be formulated as follows:

$$\min J(\theta) = \min[J1(\theta), J2(\theta), \ldots, Js(\theta)] \qquad (8)$$

subject to:

$$\theta li \leq \theta i \leq \theta ui, \ (1 \leq i \leq L) \qquad (9)$$

where $J_i(\theta)$, $i \in B := [1...s]$ are the objectives to be minimized, θ is a solution inside the L-dimensional solution space $D \subseteq R^L$, and θli and θui are the lower and the upper constraints that defined the solution space D.

The basic concept to obtain the Pareto set is known as Pareto dominance and it is defined as follows: a solution $\theta 1$ dominates another solution $\theta 2$, denoted by $\theta 1 \prec \theta 2$, if $\forall i \in B$, $J_i(\theta 1) \leq J_i(\theta 2) \wedge \exists k \in B : J_k(\theta 1) < J_k(\theta 2)$.

The Pareto set ΘP is composed by all the non-dominated solutions, and the associated Pareto front is denoted as $J(\Theta P)$. Usually, Pareto set has infinite solutions and it is very difficult to reach the exact set. Multiobjective optimization algorithm tries to obtain a well-distributed approximation ΘP^*. In this work an elitist multi-objective evolutionary algorithm is used. This algorithm is based on the concept of ε-dominance [23], named ev-MOGA [12]. Algorithm 1 shows the pseudocode of ev-MOGA. The algorithm uses three sets of solutions called populations in the context of evolutionary algorithms: A_t (to store the Pareto approximation), P_t (main population), and G_t (auxiliary population from evolutive operations).

```
1. t := 0;
2. At := Ø;
3. Pt := ini_random(D);
4. eval(Pt);
5. At := store(Pt, At);
while t < tmax do
        6. Gt := create(Pt, At);
        7. eval(Gt)
        8. At+1 := store(Gt, At);
        9. Pt+1 := update(Gt,Pt);
        10. t := t + 1;
end
```

Algorithm 1: Pseudocode of ev-MOGA.

Initially the A_t population is empty and the main population P_t is created randomly (uniform distribution). The value of the objectives for each member of the populations is calculated ("eval" function) and it is used for further dominance test. The actualization of A_t is performed with the "store" function (based on ε-dominance concept). In each iteration (evolution step) the auxiliary population G_t is obtained with individuals of A_t and P_t randomly selected, crossover and mutation operators are applied to obtain the final composition of G_t. A_t and P_t are updated with the values of G_t (applying ε-dominance and dominance respectively). When the finalization condition is achieved, the solution is Pareto set is available at A_t.

III. RESULTS

The combination of the evolutive algorithm ev-MOGA and the FDTD scheme allow us to obtain devices with high performance. However, this implies a large computational cost. Each simulation using the FDTD takes about 26 seconds in an IntelCore i7 2.8GHz. The number of calculations in an optimization process can be estimated as the number of generations multiplied by the number of new individuals at each generation plus the number of initial individuals. We have used a population of 2000 individuals for P_t and 12 new individuals are considered in each generation in G_t. tmax=600 generations, taking around 3 days of execution. After one optimization procedure, the approximated Pareto set is used as part of the initial population for the next optimization process. This iterative process is stopped when no improvements are detected at the Pareto front approximation (3 iterations have been required). The computational time for the complete process is around 9 days.

Figure 2 illustrates all the Pareto fronts including as well the reference cases of a flat panel and the BPD [6] for better comparison. It can be seen that the performance is largely increased by the optimization, regardless of the particular pair of Cost Functions used. The only exception is the case of the Cost Function J_{varlow} for which the flat panel has a value of 0. This is due to the fact that the standard deviation of the diffusion coefficient for a flat surface is 0. However it is not a good candidate because the average of that normalized diffusion coefficient is as well 1.

As a representative case, we will show here in detail only the results for the Cost Functions J_{low}&J_{varlow}. Results are illustrated in Figure 3. On the left hand side the Pareto front is plotted. The two extreme points marked with a square and a star correspond to the best individuals in the Pareto front with best performance for J_{low}(square) and J_{varlow} (star). Both individuals are represented in the central part of Figure 3. The diffusion coefficient vs frequency is plotted on the right hand side. The dashed line shows a better average performance in the low frequency range, while the continuous one shows a more homogeneous performance in that range. For frequency bands over the considered range, starting at the octave band centered in 500 Hz, a deep notch is observed.

Figure 4 compares the performance of all the Pareto front individuals obtained by means of optimization analyzed under all the pairs of Cost Functions that have been considered. Each color corresponds to the individuals optimized following a particular pair of Cost Functions. There is a case that is quite remarkable. Some of the individuals of the Pareto front optimized under J_{125}&J_{250} (marked with circles) are dominant if compare with the ones obtained with J_{low}&J_{varlow} (marked with stars) from the standpoint of this last pair of Cost Functions (left hand side plot). This make us think that the use of J_{low} and J_{varlow} has a tendency to provide optimal individuals without high average values of the diffusion coefficient, i.e., small values of J_{low}, because the algorithm loses time trying to find individuals with more homogenous diffusion coefficients through the frequency range of interest. In the rest of considered cases the dominance is fulfill by the individuals obtained with the corresponding pair of cost functions.

IV. SELECTION OF OPTIMAL INDIVIDUALS: ROBUSTNESS

In order to choose the best individual we suggest the addition of an additional criterion: robustness. This parameter measures the degree in which the values of the cost functions are affected by small changes in the cylinders that conforms the diffuser. Small changes of the values of the cylinders' radius due to mistakes in the process of manufacturing a sonic crystal, can affect to its performance, and it is very inadequate to choose one that is too sensitive to these small changes. Figure 5 illustrates this fact representing a vector in each of the Pareto front points. To create these graphs, each point of the Pareto front has been reevaluated 200 times with small random changes. Approximately 5% of the cylinders are modified (increased or decreased in radius) to simulate a defect of manufacturing. In doing so, one obtain a scattered plot. The cloud of points is averaged to a single point. Then, a vector is plotted with its origin in the considered Pareto point, and pointing to the averaged point representing the modified individuals. In all the cases, the following rule of thumb applies: The bigger the vector, the less robust the particular point is. Additionally, the decomposition of the vectors in the two components, illustrates which objective function is more likely to be deteriorated by the perturbation. For instance, it is easy to see that when optimizing with J_{low}&J_{100}, the last Cost Function is more sensitive to small variations from the original design in the manufacturing. Concerning J_{low}&J_{varlow} and J_{125}&J_{250} optimizations, one can see that the vectors are always, more or less, perpendicular to the imaginary line that runs through the Pareto front. This means that the Cost Function with better performance is usually the less robust one.

Finally, these plots can be used to choose between the individuals in the Pareto front. The idea is to choose the individuals with better robustness, which should correspond to the ones with smaller vectors. In all the plots in Figure 5 it is easy to find points that have smaller vector than the rest of candidates. Next section concerns the selection of optimal individuals using robustness as an additional criterion.

V. DISCUSSION

Traditionally, the use of several criteria in a mono-objective optimization process was achieved by averaging all the criteria to be considered. For instance in [15] two different cost functions were use, one to estimate the diffusion of a given surface averaged over the optimization frequency range, and another to avoid large variations of the diffusion in that range. In our case, this is equivalent to add the two Cost Functions so that $J=J_{low} + J_{varlow}$. In doing so, we are assigning the same relevance to both criteria J_{low} and J_{varlow}. A more general approach is to define a combined Cost Function with different ponderations for each of the Cost Functions, i.e.:

$$J = \alpha\, J_1 + (1-\alpha)\, J_2 \qquad (10)$$

In a conventional one-objective optimization using a weighted combination of Cost Functions, the relative relevance of each of the objectives has to be fixed before running the process (by means of α). On the contrary, in a multi-objective optimization, the relative relevance is stablished after the optimization process, during the decision making, when one of the individuals of the Pareto front is selected. Let us consider the extreme cases: if after the J1&J2 optimization we choose an individual on the top left of the plot of the Pareto front as the best candidate, we are prioritizing J1 over J2, while if we select an individual on the bottom right of the plot, J2 will be more important than J1. Apparently, a multiobjective optimization is equivalent to perform a multiple set of one-objective optimization with all the possible values for α. However, in doing so, not all the individuals of a Pareto Front can be found (i.e. those points are in not convex areas of the Pareto front), and eventually, these points can have additional properties, like robustness. Figure 6 illustrates this fact. All the individuals in the Pareto Fronts have been numbered from left to right and the ones that are the best candidates attending to its robustness and the average performance following equation 10 are represented. The best individual attending to its robustness is selected finding the minimum value of the Euclidian Length of the robustness vector taking into account that the two components have to be weighted with α and $(1-\alpha)$. In our particular case there are no coincidence, in other words, the best candidate attending to its robustness could never be found in a single objective optimization for whatever value of α.

VI. CONCLUSIONS

Along this paper a multiobjective optimization approach has been presented to design sound diffusers based on sonic crystals. As far as we know only single-objective has been used for diffusers design. The multiobjective approach gives the designer the possibility to consider several properties at the same time, without the need for a priori evaluations of the relevance of each criteria. Multiobjective tools give the possibility to explore different sets of solutions and help to show the trade-off between them.

Several cost functions have been used to illustrate, in the one hand, the different approaches to the problem and, in the other hand, the flexibility of multiobjective optimizations.

Additionally, we present a tool to help during the "decision making" process, based on the robustness of solutions.

Finally we have discuss the advantages of using multi-objective optimization in comparison to single-objective optimization showing that generally speaking the best individual attending to it robustness could rarely be found by single objective optimization.

REFERENCES

[1] M .R. Schroeder, "Diffuse Sound Reflection by Maximum Length Sequences", J. Acoust. Soc. Am. **57**, 149-150 (1975).

[2] T. J. Cox and P. D´antonio, *Acoustic Absorbers and Diffusers* (Taylor and Francis, New York, 2009).

[3] T. J. Cox, "Designing curved diffusers for performance spaces", Audio Eng. Soc., **44**, 354-364, (1996)

[4] M. R. Schroeder, "Towards better acoustics for concert halls", Physics Today **33**, 24-30 (1980).

[5] J. Angus, "Sound diffusers using reactive absorption grating", *Proceedings of 98th Convention Audio Engineering Society*, paper3953 (1995).

[6] J. Redondo, R. Picó Vila, V. Sánchez-Morcillo and W. Woszczyk, "Sound diffusers based on sonic crystals" J. Acoust. Soc. Am. **13**, 44412-4417 (2013).

[7] M. S. Kushwaha, P. Halevi, L. Dobrzynski and B. Djafari-Rouhani, "Acoustic band structure of periodic elastic composites", Phys. Rev. Lett. **71**, 2022-2025 (1993).

[8] R. Martínez-Sala, J. Sancho, J. V. Sánchez-Pérez, V. Gómez, J. Llinares and F. Meseguer, "Sound attenuation by sculpture", Nature **378**, 241 (1995).

[9] R. J. Hughes, J. A. S. Angus, T. J. Cox, O. Umnova, G. A. Gehring, M. Pogson, and D. M. Whittaker, "Volumetric diffusers: Pseudorandom cylinder arrays on a periodic lattice", J. Acoust. Soc. Am. **128**, 2847-2856 (2010).

[10] V. Romero-García, E. Fuster, L. M. García-Raffi, E. A. Sánchez-Pérez, M. Sopena, J. Llinares, and J. V. Sánchez-Pérez, "Band gap creation using quasiordered structures based on sonic crystals", Appl. Phys. Lett. **88**, 174104 (2006).

[11] V. Romero-García, J. V. Sánchez-Pérez, L. M. García-Raffi, J. M. Herrero, S. García-Nieto, and X. Blasco "Hole distribution in phononic crystals: Design and optimization" J. Acoust. Soc. Am. **125**, 3774-3783 (2009).

[12] J. M. Herrero, S. García-Nieto, X. Blasco, V. Romero-García, J. V. Sánchez-Pérez and L. M. Garcia-Raffi, "Optimization of sonic crystal attenuation properties by ev-MOGA multiobjective evolutionary algorithm", Struct. Multidisc. Optim. **39**, 203-215 (2009)

13 A. Hakansson, J. Sánchez-Dehesa, and L. Sanchis, "Acoustic lens design by genetic algorithms", Phys. Rev. B **70**, 214302 (2004).

[14] L. Sanchis, A. Hakansson, D. López-Zanón, J. Bravo-Abad, and J. Sánchez-Dehesa, "Integrated optical devices design by genetic algorithm", Appl. Phys. Lett. **84**, 4460 (2004).

[15] T. J. Cox, "The optimization of profiled diffusers", J. Acoust. Soc. Am. **97**, 2928-2936 (1995).

[16] ISO 17497-1:2004, *Acoustics Sound-Scattering Properties of Surfaces, Part 1: Measurement of the Random-Incidence Scattering Coefficient in a Reverberation Room* (International Standards Organization, Geneva, Switzerland, 2004).

[17] ISO 354:2003, Acoustics - *Measurement of sound absorption in a reverberation room* (International Standards Organization, Geneva, Switzerland, 2004).

[18] ISO 17497-2:2012, Acoustics - *Measurement of Sound Scattering Properties of Surfaces, Part 2: Measurement of the Directional Diffusion Coefficient in a Free Field* (International Standards Organization, Geneva, Switzerland, 2003).

[19] J. Redondo, R. Picó, B. Roig and M. R. Avis, "Time domain simulation of sound diffusers using finite-difference schemes", Acta Acust. Acust. **93**, 611-622 (2007).

[20] J. Redondo, R. Picó, M. R. Avis and T. J. Cox, "Prediction of the Random-Incidence Scattering Coefficient Using a FDTD Scheme", Acta Acust. Acust. **95**, 1040-1047 (2009)

[21] K. M. Miettinen, *Nonlinear multiobjective optimization* (Kluwer Academic Publishers, Boston, Massachusetts, 1998).

[22] C. Coello, D. Veldhuizen and G. Lamont, *Evolutionary algorithms for solving multi-objective problems* (Kluwer Academic Publishers, New York, 2002).

[23] M. Laumanns, L. Thiele, K. Deb and E. Zitzler, "Combining convergence and diversity in evolutionary multi-objective optimization". Evol. Comput. **10**, 263-282 (2002).

FIGURE CAPTIONS

Figure 1: a) Schematic configuration of the Bi-Periodic sonic crystal sound diffuser (BPD); b) Example of genetic codification

Figure 2. (COLOR ONLINE) Pareto fronts for the three pairs of Cost Functions (BPD and flat panel are as well plotted for comparison). a) J_{low}&J_{varlow}; b) J_{125}&J_{250}; c) J_{low}&J_{100}.

Figure 3. (COLOR ONLINE) a) Pareto front for the Cost Functions J_{low}&J_{varlow}. b): The optimized sonic crystal corresponding to the two extreme values of the Pareto front (Best individual for J_{varlow} marked with a star. Best individual for J_{low} marked with a square). c): Diffusion coefficient of both individuals.

Figure 4. (COLOR ONLINE) Detailed view of Figure 3 adding the Pareto fronts of all the pairs of Cost Functions. a*) J_{low}&J_{varlow}; b) J_{125}&J_{250}; c) J_{low}&J_{100}.*

Figure 5. Pareto fronts with the Robustness vectors for the three pairs of Cost Functions considered. a) J_{low}&J_{varlow}; b) J_{125}&J_{250}; c) J_{low}&J_{100}.

Figure 6. Best individuals as a function of α (See eq. 10), attending to: Weighted average, solid line; Robustness, dotted line. From left to right: J_{low} & J_{varlow}, J_{125} & J_{250} and J_{low} & J_{100}.

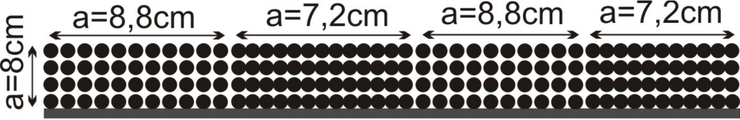

(a)

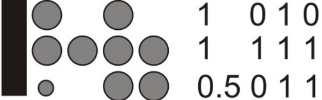

$$\theta = (1, 0, 1, 0, 1, 1, 1, 1, 0.5, 0, 1, 1)$$

(b)

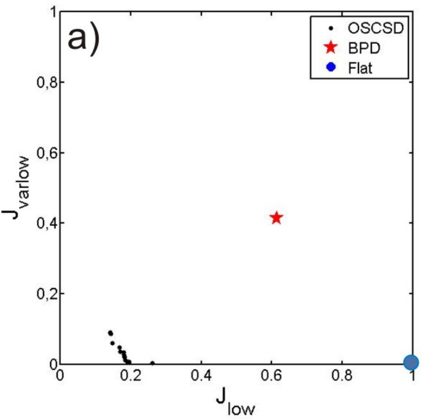
a)
OSCSD
BPD
Flat
J_{varlow}
J_{low}
1
0,8
0,6
0,4
0,2
0
0
0.2
0.4
0.6
0.8
1

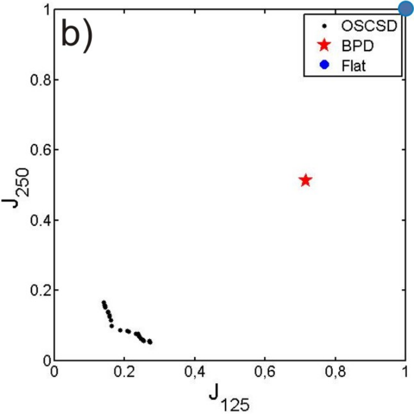

b)
OSCSD
BPD
Flat
J_{250}
J_{125}
0
0.2
0.4
0.6
0.8
1
0
0.2
0,4
0,6
0,8
1

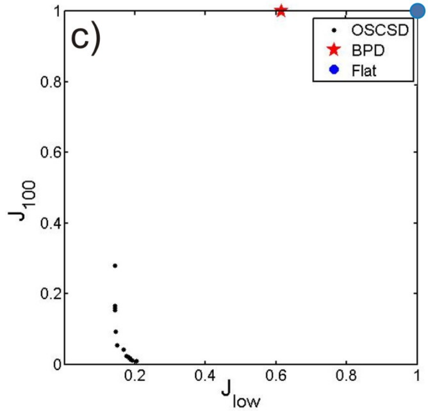

c)
OSCSD
BPD
Flat
1
0.8
0.6
0.4
0.2
0
J_{100}
0.2
0.4
0.6
0.8
1
J_{low}

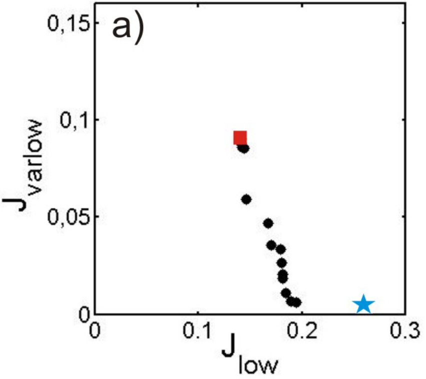

a)
0,15
0,1
0,05
0
J varlow
0
0.1
0.2
0.3
J low

b)

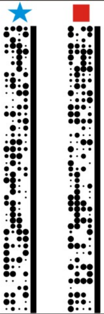

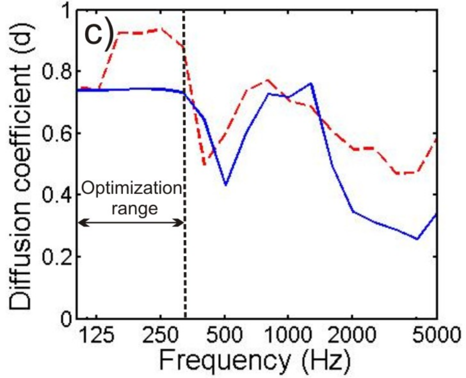

c)
Diffusion coefficient (d)
1
0.8
0.6
0.4
0.2
0
Optimization
range
125
250
500
1000
2000
5000
Frequency (Hz)

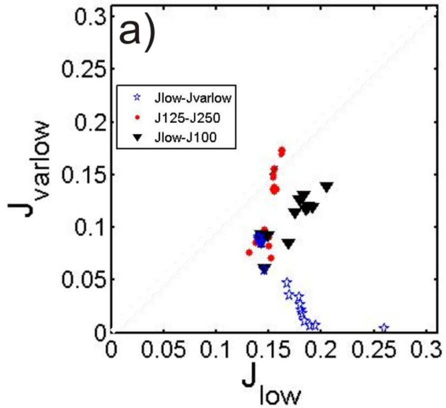

a)
Jlow-Jvarlow
J125-J250
Jlow-J100
J_{varlow}
J_{low}
0
0.05
0.1
0.15
0.2
0.25
0.3

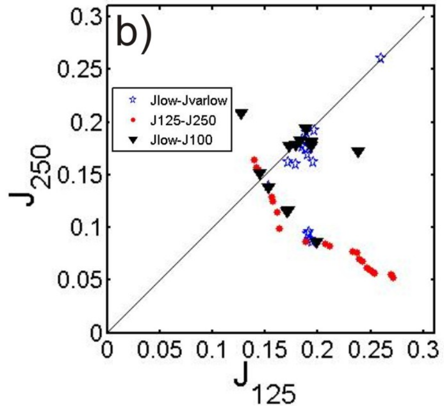

b)
Jlow-Jvarlow
J125-J250
Jlow-J100
J_{250}
J_{125}
0
0.05
0.1
0.15
0.2
0.25
0.3

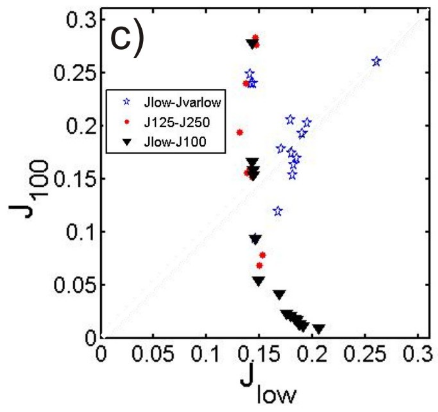

c)
Jlow-Jvarlow
J125-J250
Jlow-J100
0.3
0.25
0.2
0.15
0.1
0.05
0
0
0.05
0.1
0.15
0.2
0.25
0.3
J_{100}
J_{low}

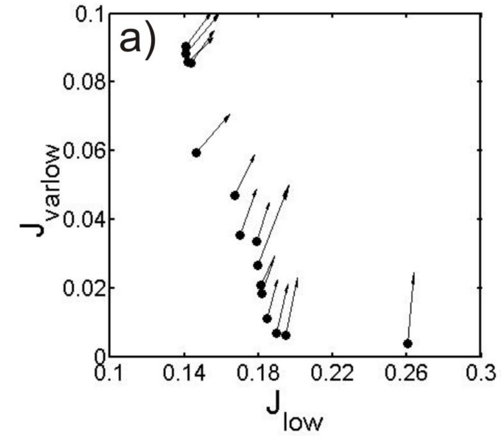

a)
0.1
0.08
0.06
0.04
0.02
0
J varlow
0.1
0.14
0.18
0.22
0.26
0.3
J low

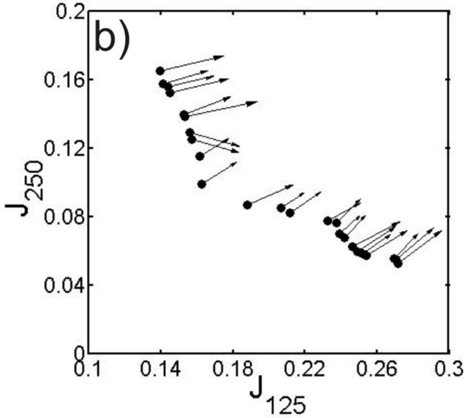
b)
0.2
0.16
0.12
0.08
0.04
0
J_{250}
0.1
0.14
0.18
0.22
0.26
0.3
J_{125}

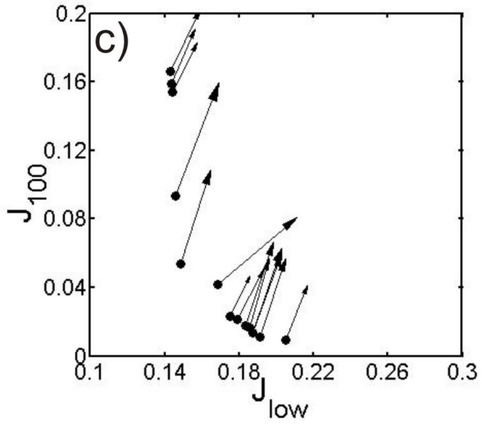
c)
0.2
0.16
0.12
0.08
0.04
0
J_{100}
0.1
0.14
0.18
0.22
0.26
0.3
J_{low}

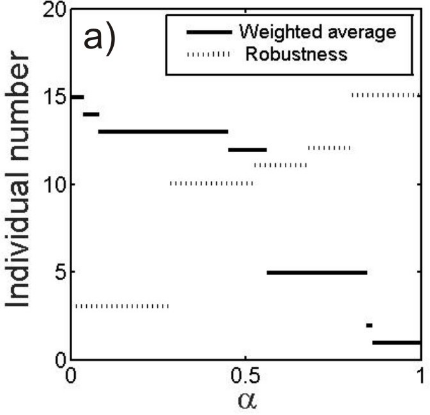
a)
Weighted average
Robustness
Individual number
α
0
0.5
1
5
10
15
20

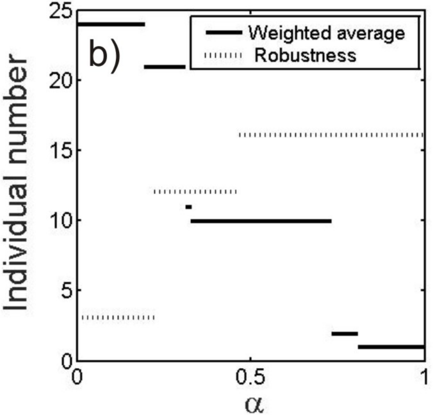
b)
Weighted average
Robustness
Individual number
α
0
5
10
15
20
25
0
0.5
1

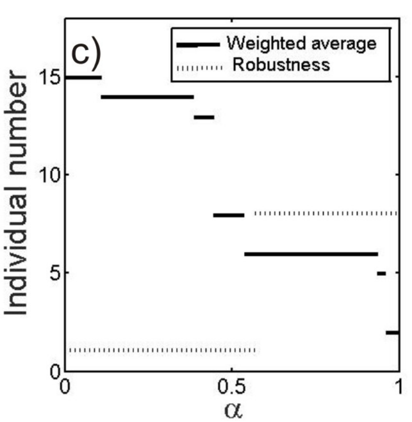
c)
Weighted average
Robustness
Individual number
15
10
5
0
0
0.5
1
α